

## Similarity in Calcium Channel Activity of Annexin V and Matrix Vesicles in Planar Lipid Bilayers

Nelson Arispe,\* Eduardo Rojas,\* Brian R. Genge,# Licia N. Y. Wu,# and Roy E. Wuthier#

\*Laboratory of Cell Biology and Genetics, National Institute of Diabetes, Digestive, and Kidney Diseases, National Institutes of Health, Bethesda, Maryland 20892, and #Department of Chemistry and Biochemistry, and the School of Medicine, Laboratory for Biomaterialization Research, University of South Carolina, Columbia, South Carolina 29208 USA

**ABSTRACT** Matrix vesicles (MVs), structures that accumulate  $\text{Ca}^{2+}$  during the initiation of mineral formation in growing bone, are rich in annexin V. When MVs are fused with planar phospholipid bilayers, a multiconductance  $\text{Ca}^{2+}$  channel is formed, with activity essentially identical to that observed when annexin V is delivered to the bilayer with phosphatidylserine liposomes.  $\text{Ca}^{2+}$  currents through this channel, from either MV or annexin V liposomes, are blocked by  $\text{Zn}^{2+}$ , as is  $\text{Ca}^{2+}$  uptake by MV incubated in synthetic cartilage lymph. Blockage by  $\text{Zn}^{2+}$  was most effective when applied to the side containing the MV or liposomes. ATP and GTP differentially modulated the activity of this channel: ATP increased the amplitude of the current and the number of conductance states; GTP dramatically reduced the number of events and conductance states, leading to well-defined  $\text{Ca}^{2+}$  channel activity from either MV or the annexin V liposomes. In the distinctive effects of ATP, GTP, and  $\text{Zn}^{2+}$  on the  $\text{Ca}^{2+}$  channel activity observed in both the MV and the liposome systems, the common factor was the presence of annexin V. From this we conclude that  $\text{Ca}^{2+}$  entry into MV results from the presence of annexin V in these membrane-enclosed structures.

### INTRODUCTION

Matrix vesicles are membrane-enclosed extracellular microstructures that are directly involved with the induction of calcium phosphate mineral deposition in a wide variety of newly developing vertebrate hard tissues (Anderson, 1969; Bonucci, 1970).  $\text{Ca}^{2+}$  uptake by isolated MVs, when incubated in a synthetic cartilage lymph, follows a predictable kinetic sequence in which after a lag period there is a rapid accumulation of mineral ions, followed by a period of slower uptake (Wuthier, 1988). The rate of mineralization by isolated MVs can be stimulated by incubation with *o*-phenanthroline, a  $\text{Zn}^{2+}$  chelator. Conversely,  $\text{Zn}^{2+}$  has been shown to block  $\text{Ca}^{2+}$  uptake by MVs (Sauer et al., 1989). Recent work has identified two key components required for MV function in the induction of crystalline mineral formation in vitro. One is an acid-labile, intraluminal nucleational core (Wu et al., 1993; McLean et al., 1987; Valhmu et al., 1990), and the other is  $\text{Ca}^{2+}$  entry pathways (Register et al., 1984; Genge et al., 1988; Kirsch and Wuthier, 1994) to allow its accumulation in the MV.

One of the dominant groups of constitutive proteins present in MVs are the annexins (Genge et al., 1989, 1990). Annexins II and V are particularly abundant (Genge et al., 1990, 1991, 1992), although annexin VI is also present in significant amounts (Cao et al., 1993). Recent studies by Rojas et al. (1990, 1992) and others (Berendes et al., 1993;

Demange et al., 1994) have demonstrated that annexin V incorporated into lipid bilayer membranes exhibits  $\text{Ca}^{2+}$  channel activity. These findings are complementary to the three-dimensional crystalline structural analyses of human (Huber et al., 1990; Burger et al., 1994) and avian (Bewley et al., 1993) annexin V that showed the presence of a hydrophilic core through the protein formed by surrounding parallel  $\alpha$ -helices.

In the work now reported we examined the characteristics of the  $\text{Ca}^{2+}$  channels resident in MVs and show for the first time that they are essentially identical to those of annexin V. We also show here that GTP is a powerful modulator of both the conductance and gating of the channel. Because the responses of the reconstituted  $\text{Ca}^{2+}$  channel to a variety of modulators are remarkably similar in both the MV and annexin V-liposome systems, these findings strongly support the hypothesis that  $\text{Ca}^{2+}$  uptake by MVs is mediated by the activity of annexin V, a dominant protein in these structures. This is the first clear demonstration of a physiological function for annexin V in any biological system. Furthermore, our finding that annexin V channel gating is modulated by  $\text{Zn}^{2+}$ , ATP, and GTP raises the distinct possibility that these endogenous factors are important regulators of MV  $\text{Ca}^{2+}$  channel activity in vivo.

Received for publication 6 May 1996 and in final form 16 July 1996.

Address reprint requests to Dr. Roy E. Wuthier, Department of Chemistry and Biochemistry, University of South Carolina, Laboratory for Biomaterialization Research, 424A Physical Sciences Center, Columbia, SC 29208. Tel.: 803-777-6626; Fax: 803-777-9521; E-mail: wuthier@psc.sc.edu.

© 1996 by the Biophysical Society  
0006-3495/96/10/1764/12 \$2.00

### MATERIALS AND METHODS

#### Avian matrix vesicle isolation and annexin V purification studies

The experiments involving calcium uptake by avian matrix vesicles and purification of avian annexin V were carried out at the University of South Carolina.

## Isolation of collagenase-released matrix vesicles

Native matrix vesicles capable of inducing the formation of calcium phosphate mineral phase were isolated from the growth plate of 6–8-week-old broiler-strain chickens by two different methods. Trypsin-collagenase-released MVs (TCRMVs) were isolated as described by Genge et al. (1988), and hyaluronidase-collagenase-released MVs (HCRMVs) were prepared by a modification of the method of Kirsch et al. (1994).

## Calcium uptake by MVs

MV mineral formation was assessed by measuring the accumulation of mineral ions from SCL. Ca<sup>2+</sup> uptake was assayed by monitoring the change in relative turbidity based on the method of Brecevic and Füredi-Milhofer (1972). In brief, 160  $\mu$ l of MV samples was added to 96-well half-area microtiter plates (Costar Corp., Cambridge, MA) and incubated at 37°C in a Labsystems IEMS Reader MF. At timed intervals, absorbance readings were measured at 340 nm, and the percentage of calcium uptake was derived from the relative turbidity, where the change of 0.01 in absorbance at 340 nm corresponded to  $\sim$ 1.2% Ca<sup>2+</sup> uptake.

## Purification of avian annexin V from MV

Annexin V was purified from MV-enriched microsomes (Wuthier et al., 1978) by the method of Genge et al. (1990). In brief, the pellet was resuspended in buffer (in mM: 100 NaCl, 10 TrisCl, 5 CaCl<sub>2</sub>, 0.2 phenylmethylsulfonyl fluoride, 6 benzamide, pH 7.4) containing 1% Triton X-100 (final protein concentration of 5.0 mg/ml). After centrifugation at 4°C for 20 min at 240,000  $\times$  g, the supernatant was removed and the pellet was extracted by homogenization in low-ionic-strength, EGTA-containing buffer (in mM: 10 NaCl, 5 EGTA, 20 sodium acetate, pH 5.6) followed by incubation for 5 min at 4°C. After centrifugation as above, the supernatant fraction, enriched in the 33-kDa annexin V, was applied directly to a cation exchange column (FPLC Mono S HR 5/5; Pharmacia Fine Chemicals, Piscataway, NJ) equilibrated with a sodium acetate (20 mM) solution at pH 5.6. The column was eluted with a 15-ml NaCl gradient from 0 to 280 mM (40- $\mu$ l samples were taken for sodium dodecyl sulfate-polyacrylamide gel electrophoretic (SDS-PAGE) analysis). Highly purified 33-kDa annexin V eluted as a single peak between 150 and 180 mM NaCl was used for ion channel studies.

## Ca<sup>2+</sup> channel reconstitution studies

Ca<sup>2+</sup> channel reconstitution studies were carried out at the National Institutes of Health.

## Bilayer membranes

The methods used in our channel reconstitution studies have been described elsewhere (Arispe et al., 1992). In brief, the experimental chamber consisted of two compartments separated by a thin teflon film. The solutions in the compartments were electrically connected to the input of a voltage clamp amplifier via agar bridges (2% agar in 0.5 M KCl) and Ag/AgCl pellet electrodes. Channel currents were recorded using a patch-clamp amplifier (Axopatch-1D; Axon Instruments) equipped with a low-noise headstage (CV-4B) specially designed for lipid bilayer membrane work. Permanent records of the current and commanded voltages were made on digital magnetic tapes using a PCM/VCR digital system with a frequency response in the range of 0–25,000 Hz.

Planar lipid bilayers were formed as described by Wonderlin et al. (1990). In brief, a suspension of synthetic 1-palmitoyl-2-oleoyl-phosphatidylethanolamine (PE) and phosphatidylserine (PS) (Avanti Polar Lipids, Alabaster, AL), 1:1 in *n*-decane (20  $\mu$ g each/ $\mu$ l), was prepared. With a small plastic spatula, a tiny volume of this suspension was delivered to the

hole ( $\sim$ 100–150- $\mu$ m diameter) across the thin teflon membrane separating two compartments filled with solutions.

## Incorporation of matrix vesicle ion channels

To fuse native MVs with the lipid bilayer membrane, a suspension of MVs (0.5 mg protein/ml) in SCL containing 1 mM Ca<sup>2+</sup> was prepared. Ion channels present in the MV membrane were incorporated into the bilayer by adding a small volume (6–12  $\mu$ l) of this suspension to one of the compartments (*cis*) of the bilayer chamber. Spontaneous fusion of matrix vesicles with the bilayer membrane occurred after the chamber solution was stirred with teflon-coated magnets.

## Annexin V channel activity

A solution of highly purified avian annexin V (0.5  $\mu$ g/ $\mu$ l) in sodium acetate buffer (20 mM, pH 5.6, containing 180 mM NaCl and 45  $\mu$ M CaCl<sub>2</sub>) was introduced into a suspension of pure PS liposomes. To prepare the liposomes, 25  $\mu$ l of PS dissolved in CHCl<sub>3</sub> (10 mg/ml) was placed in a tube. After evaporation of the solvent by blowing N<sub>2</sub> gas, a small volume (50  $\mu$ l) of 1 M potassium aspartate (pH 7.2) was added, and the resulting mixture was sonicated for 5 min. Next an aliquot (5  $\mu$ l) of the stock solution of avian annexin V was added to the liposomal suspension, and the combination was sonicated for an additional period of 2 min. A sample (6–12  $\mu$ l) of the liposomal suspension containing the annexin V protein ( $\sim$ 1  $\mu$ g) was added to the solution on the *cis* side of the chamber and stirred.

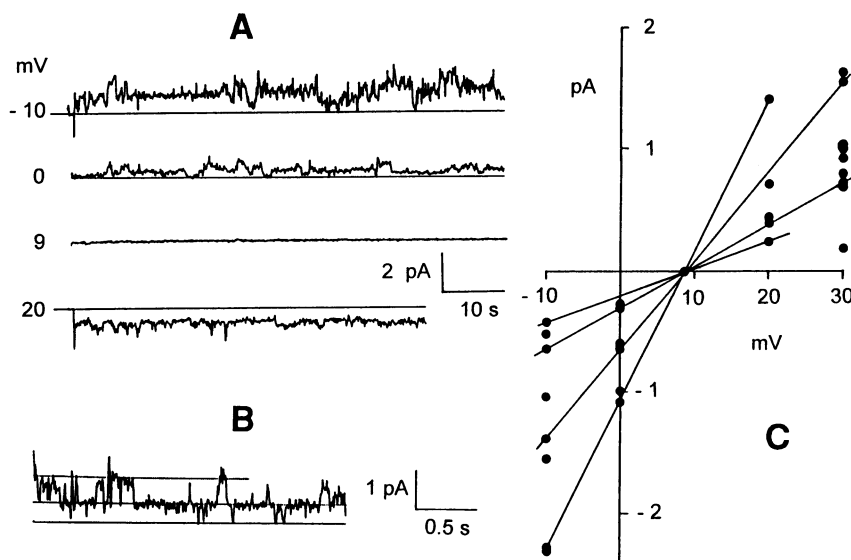
## RESULTS

### Specificity of the Ca<sup>2+</sup> channel activity in MV

Annexin V, one of the major MV proteins, forms Ca<sup>2+</sup>-selective channels across planar phospholipid bilayer membranes (Rojas et al., 1992). To test the hypothesis that annexin V provides the Ca<sup>2+</sup> entry pathway in these vesicles, TCRMVs prepared for Ca<sup>2+</sup> uptake study were allowed to fuse with acidic phospholipid bilayer membranes. Using an asymmetrical CsCl solution system (200 mM in the *trans* side; 100 mM in the *cis* side), as depicted in Fig. 1 A, the current record at 0 mV revealed the presence of channel activity. Because the chemical gradient was the same for both Cs<sup>+</sup> and Cl<sup>−</sup>, positive currents identify Cs<sup>+</sup> as the charge carrier moving down its gradient from the *trans* to the *cis* side. Adjusting the transmembrane potential to 9 mV (*cis* side positive) made the current record virtually silent. The electrical potential gradient balanced the chemical potential gradient for the positive Cs<sup>+</sup> ions and thus minimized the net flow of Cs<sup>+</sup>. From this equilibrium potential of 9 mV, we estimate that Cs<sup>+</sup> is 3.25 times more permeable than Cl<sup>−</sup> through the open channel. These data, which were confirmed in 13 additional incorporations under the same ionic conditions, led us to conclude that the cation-selective channel expressed in the bilayer is indeed a MV membrane resident channel.

The current records depicted in Fig. 1 A contained periods of regular activity, and the record shown in Fig. 1 B reveals well-defined levels (0.52 and 1.04 pA at  $-$ 10 mV), which were used to construct the current-voltage diagram in Fig. 1 C. Values measured at different potentials were connected by straight lines; all crossed the horizontal axis at 9 mV.

FIGURE 1 Cation-channel activity reconstituted from TCRMVs. TCRMVs were allowed to fuse with the PS:PE bilayer separating an asymmetrical solution system (100 mM CsCl in the *cis* compartment; 200 mM CsCl in the *trans* compartment). (A) Cation channel activity at different membrane potentials (-10, 0, 9, and 20 mV, indicated on the left). (B) Segment from the record at -10 mV on an expanded scale to show well-defined conductance levels. (C) Current-voltage relationships were obtained by drawing straight lines crossing the potential axis at 9 mV. Slope conductances were estimated as 22, 34, 73, and 127 pS.



Thus, the range of conductance levels (from 22 to 127 pS) displayed by the TCRMV channel incorporated into the bilayer corresponds to a channel with a fixed  $\text{Cs}^+/\text{Cl}^-$  selectivity ratio.

### Similarity between MV and annexin V $\text{Ca}^{2+}$ channels

Fig. 2 A depicts two records of the channel activity at -40 mV (upper) and 40 mV (lower) when MVs were fused with the bilayer membrane. This channel activity was recorded using an asymmetrical solution system with 70 mM  $\text{CaCl}_2$  in the *trans* side and 140 mM NaCl in the *cis* side. The dotted horizontal line represents zero current. At -40 mV, upward deflections of the trace correspond to a flow of positive charges ( $\text{Ca}^{2+}$ ) from the *trans* to the *cis* side. At 40 mV, downward deflections correspond to a flow of positive charges ( $\text{Na}^+$ ) moving from the *cis* to the *trans* side. MV channel activity in experiments using the impermeable anion HEPES<sup>-</sup> in place of  $\text{Cl}^-$ , but maintaining the cations (140 mM  $\text{Na}^+$  and 70 mM  $\text{Ca}^{2+}$ ), was very similar to that in Figs. 1 and 2 A (data not shown). From this we conclude that the MV channel incorporated into the bilayer is permeable to  $\text{Ca}^{2+}$ , as well as  $\text{Cs}^+$  and  $\text{Na}^+$ , and is much less permeable to anions.

Similar experiments were carried out when liposomes containing annexin V were fused to the bilayer membrane. Fig. 2 B shows a record of the annexin V channel activity made in the presence of symmetrical CsHEPES (200 mM) solutions with no added  $\text{Ca}^{2+}$ . Because  $\text{Cs}^+$  is the only permeable ion present in the system, it is clear that avian annexin V channel is also permeable to  $\text{Cs}^+$ , in good agreement with previous observations made with highly purified human annexin V (Rojas et al., 1990).

A distinctive feature, common to both MV (Fig. 2 A) and annexin V (Fig. 2 B) channels, is the irregular pattern of channel events. The lower records of both figures depict segments indicated by the horizontal bars beneath the upper

records. On these expanded time bases, well-defined channel openings and complete closures are readily discernible, indicating that the irregular activity of both the MV and annexin V channels is the result of multiple transitions between closed and different open conformations of the channel. This behavior indicates the presence of a single, multiple-conductance channel attributable to annexin V in both bilayer preparations.

### $\text{Zn}^{2+}$ inhibits both $\text{Ca}^{2+}$ uptake by MVs and channel activity of MVs

Previous studies (Sauer et al., 1989) demonstrated that  $\text{Zn}^{2+}$  has a profound inhibitory effect on  $\text{Ca}^{2+}$  uptake by MVs incubated in SCL. In these studies, the isolated MV rapidly accumulated  $\text{Ca}^{2+}$  and  $\text{P}_i$  and induced the formation of mineral. As expected, the presence of  $\text{Zn}^{2+}$  in SCL completely inhibited  $\text{Ca}^{2+}$  uptake by MVs (Fig. 3 A). Similarly, the  $\text{Ca}^{2+}$  channel activity of MVs was also inhibited by  $\text{Zn}^{2+}$  (Fig. 3 B). The multiconductance flickering  $\text{Ca}^{2+}$  channel activity seen in records B-1 and B-2 became quenched immediately after the addition of  $\text{Zn}^{2+}$  to both the *cis* and *trans* compartments (indicated by the arrow, record B-3). The  $\text{Ca}^{2+}$  current remained blocked thereafter (record B-4). It should be noted that high levels of  $\text{Zn}^{2+}$  (1–2 mM) were required only if a high concentration of  $\text{Ca}^{2+}$  (70 mM) was present on the *cis* side (symmetrical 70 mM  $\text{CaCl}_2$  for Fig. 3 B). In contrast, in the presence of symmetrical 200 mM Cs-HEPES, a 10-fold lower level of  $\text{Zn}^{2+}$  was sufficient to block the channel. Previous studies by Rojas et al. (1992) had demonstrated that  $\text{Zn}^{2+}$  strongly inhibits the  $\text{Ca}^{2+}$  channel activity of annexin V.

### ATP activates MV $\text{Ca}^{2+}$ channel activity

Another factor, tested as a modulator of  $\text{Ca}^{2+}$ -channel activity in MVs, was the nucleotide triphosphate ATP. This

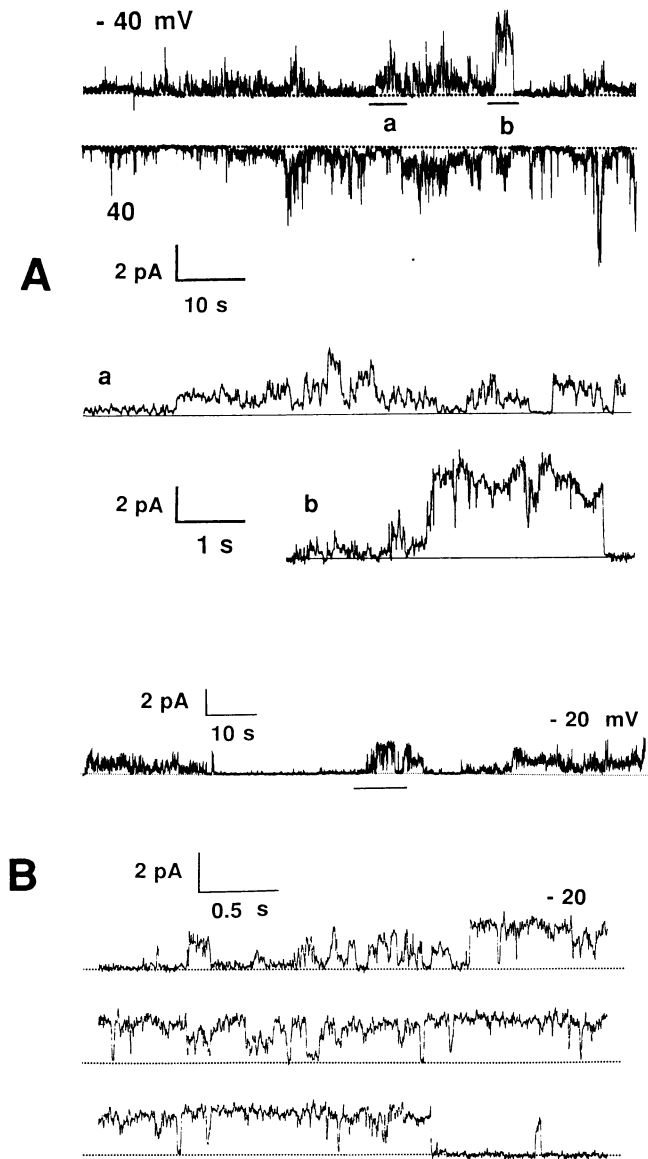


FIGURE 2 Comparison of cation channel activities of MV and annexin V incorporated into planar acidic phospholipid bilayer membranes. (A) TCRMVs were allowed to fuse with a PS:PE bilayer separating an asymmetrical solution system (140 mM NaCl in the *cis* compartment and 70 mM CaCl<sub>2</sub> in the *trans* compartment). A shows two records at -40 mV (upper) and +40 mV (lower) tracing. The underlined segments (a and b) are shown below in an expanded time scale to more clearly reveal the irregular pattern of channel events. (B) Liposomes containing pure chicken annexin V were fused to a PS:PE bilayer separating a symmetrical solution system (200 mM CsHEPES in both *cis* and *trans* chambers). The underlined segment in the upper tracing is shown in an expanded time scale in the three tracings shown below. Note the close similarity in the flickering type of current displayed in both the TCRMV and annexin V preparations. The irregular, multiconductance activity of the cation channel is characteristic of that seen previously with the annexins (Rojas et al., 1990).

nucleotide had been reported to stimulate Ca<sup>2+</sup> uptake in some MV preparations (Hsu, 1992). Accordingly, we studied the effect of ATP on MV Ca<sup>2+</sup> channel activity. Fig. 4 demonstrates the stimulation that occurs when ATP (20

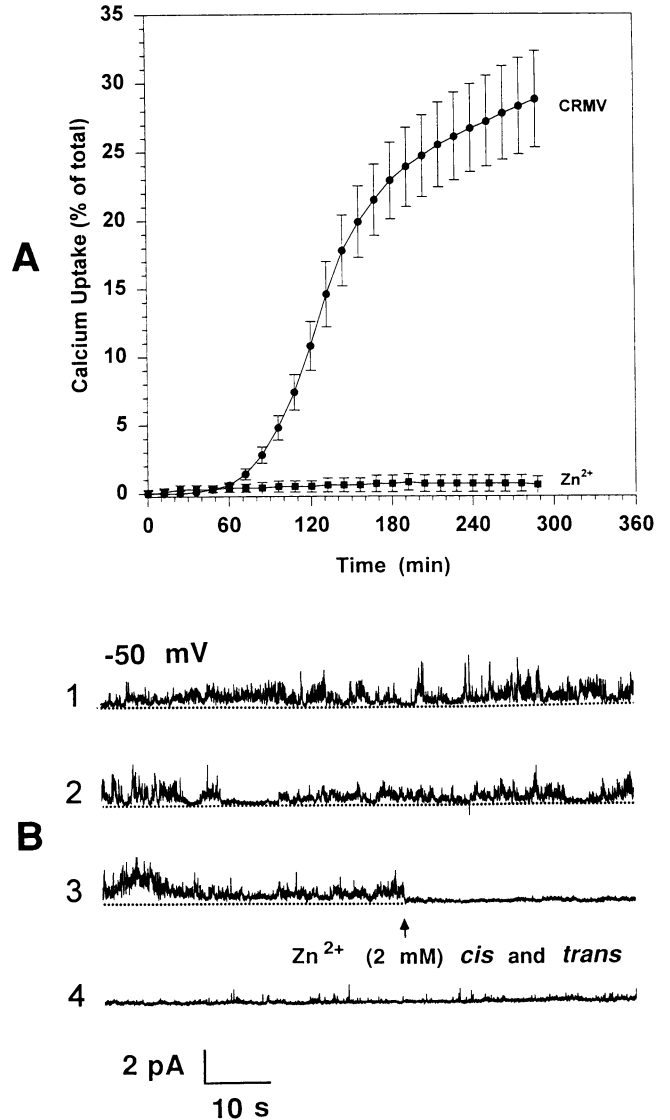


FIGURE 3 Zn<sup>2+</sup> inhibits Ca<sup>2+</sup> uptake by MV, and blocks MV Ca<sup>2+</sup> channel activity. (A) MV Ca<sup>2+</sup> uptake assays were performed by turbidometric assay, as described in Materials and Methods. TCRMVs were used, and Zn<sup>2+</sup> (20 μM) was added to the SCL (2.0 mM Ca<sup>2+</sup>) in the incubations shown in the lower tracing. Values shown are the mean ± SD of six replicate samples. Note the profound inhibition of Ca<sup>2+</sup> uptake by the MV produced by the addition of Zn<sup>2+</sup> to the SCL. (B) TCRMV channel activity was measured using a symmetrical solution system (70 mM CaCl<sub>2</sub> in both *cis* and *trans* chambers). The arrow beneath record 3 indicates the time of addition of 2 mM Zn<sup>2+</sup> to both the *cis* and *trans* compartments. Note the similar flickering ion current (records 1 and 2), and the immediate and profound inhibition of Ca<sup>2+</sup> channel activity produced by the addition of Zn<sup>2+</sup> to this system (records 3 and 4).

μM) is applied on the *cis* side of the membrane. The segments of current shown in Fig. 4 A illustrate the channel activity of control MV with Cs<sup>+</sup> as the charge carrier in a symmetrical solution system (200 mM CsHEPES on both sides) acquired at both -80 mV and -40 mV. Fig. 4 B demonstrates the stimulation of MV channel activity at -80 mV that occurs within minutes after the addition of ATP.

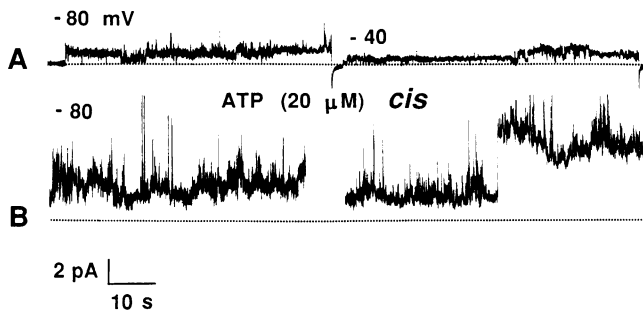


FIGURE 4 Effects of ATP on TCRMV channel activity. TCRMV channel activity was measured using a symmetrical solution system in which 200 mM CsHEPES was present in both the *cis* and *trans* compartments. MV  $\text{Ca}^{2+}$  channel activity was recorded for more than 1 min first at  $-80$  mV and then at  $-40$  mV (A) to establish the current pattern of this preparation. Approximately 1 min after the addition of ATP ( $20 \mu\text{M}$ ) to the *cis* chamber, the potential was returned to  $-80$  mV and then reestablished (B). Note the marked increase in the amplitude of the cation current activity after addition of ATP to the *cis* side.

Note the marked increase in amplitude and activity of the cation channel in the presence of ATP.

### Antagonistic action of ATP on $\text{Zn}^{2+}$ -induced blockade and directionality of this blockade

The observation that external application of micromolar levels of  $\text{Zn}^{2+}$  can effectively block  $\text{Ca}^{2+}$  uptake by MVs (Sauer et al., 1989; see also Fig. 3 A) suggests that the molecular complex involved in  $\text{Ca}^{2+}$  influx has a  $\text{Zn}^{2+}$ -binding domain exposed to the external aspect of the MV membrane. Furthermore, because ATP stimulated the MV  $\text{Ca}^{2+}$  channel, whereas  $\text{Zn}^{2+}$  strongly blocked it, one might expect to observe antagonism between these two effectors. One would expect the most effective blockade to occur when  $\text{Zn}^{2+}$  is added to the compartment from which the MVs fused to the bilayer membrane. To test the validity of this prediction, we studied the interaction between these two effectors in both asymmetrical (Fig. 5 A) and symmetrical (Fig. 5 B) solution systems. Fig. 5 A depicts current records acquired at two transmembrane potentials,  $-40$  mV (record A-1) and  $40$  mV (record A-2), with  $1 \text{ mM Zn}^{2+}$  applied to the *trans* side and  $2 \text{ mM ATP}$  applied to the *cis* side. In this asymmetrical system ( $140 \text{ mM NaCl}$  on the *cis* side,  $70 \text{ mM CaCl}_2$  on the *trans* side)  $\text{Ca}^{2+}$  is the main charge carrier for negative potentials, whereas  $\text{Na}^+$  is the main charge carrier at positive potentials. Note in Fig. 5 A that the presence of ATP maintains the MV channel in an active conformation, despite the presence of  $\text{Zn}^{2+}$  in the *trans* side. The antagonistic effects of ATP and  $\text{Zn}^{2+}$  were also studied with  $\text{Cs}^+$  as the charge carrier in a symmetrical solution system ( $200 \text{ mM CsHEPES}$  on both sides; Fig. 5 B) with  $\text{Zn}^{2+}$  applied to the *cis* side. Notice here that although  $\text{Zn}^{2+}$  had no noticeable effect on the ATP-stimulated MV channel activity at  $-80$  mV (Fig. 5 B-1) where  $\text{Cs}^+$  was moving from the *trans* to the *cis* side, it clearly inhibited ATP-stimulated MV channel currents carried by  $\text{Cs}^+$  moving from *cis* to *trans*

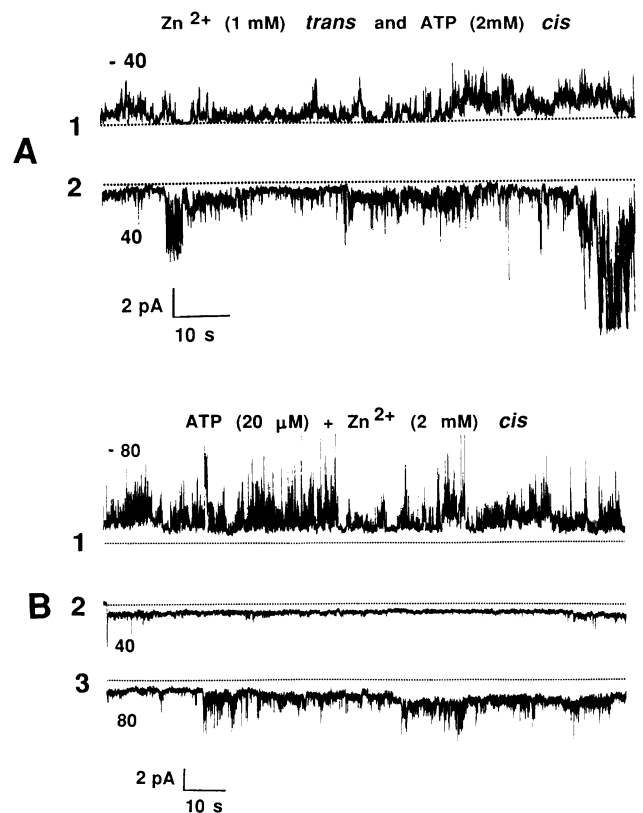
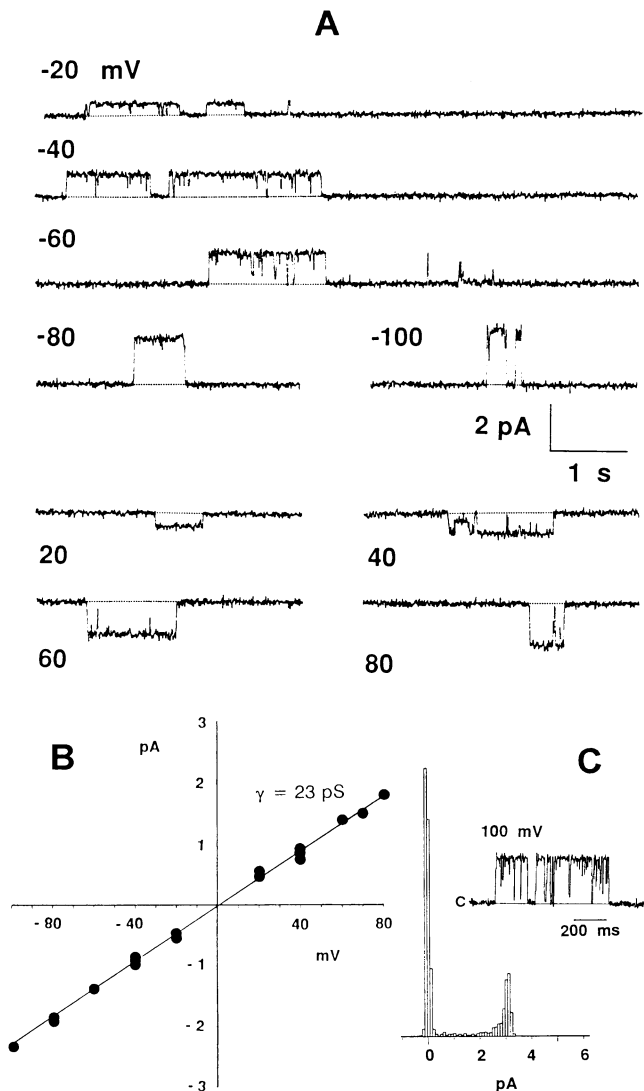


FIGURE 5 Antagonistic action of ATP on  $\text{Zn}^{2+}$ -induced blockade. Interactions between ATP and  $\text{Zn}^{2+}$  on MV cation channel activity were studied in both asymmetrical ( $140 \text{ mM NaCl}$ , *cis* compartment;  $70 \text{ mM CaCl}_2$ , *trans* compartment) and symmetrical ( $200 \text{ mM CsHEPES}$ , both compartments) systems. In these experiments the effects were examined when ATP and  $\text{Zn}^{2+}$  were present together on the same side, or when they were on opposite sides of the membrane. In the asymmetrical system (A), ATP ( $2 \text{ mM}$ ) was added to the *cis* and  $\text{Zn}^{2+}$  ( $1 \text{ mM}$ ) was added to the *trans* compartment. The potential was set at either  $-40$  mV, in which  $\text{Ca}^{2+}$  was the charge carrier from the *trans* to the *cis* compartment (A-1), or  $+40$  mV, in which  $\text{Na}^+$  was the charge carrier from the *cis* to the *trans* compartment. Note in this system that ATP in the *cis* compartment overcame the effect of the  $\text{Zn}^{2+}$  on the *trans* side in blocking movement of either  $\text{Ca}^{2+}$  or  $\text{Na}^+$ . In the symmetrical system (B) both ATP ( $20 \mu\text{M}$ ) and  $\text{Zn}^{2+}$  ( $2 \text{ mM}$ ) were present together on the *cis* side, and current was measured at  $-80$  mV (B-1) and at  $+40$  and  $+80$  mV (B-2 and B-3). Note the marked stimulatory effect of ATP, and the lack of effect of  $\text{Zn}^{2+}$  applied on the *cis* side, on movement of  $\text{Cs}^+$  from the *trans* to the *cis* side. In contrast, in B-2 and B-3, at  $+40$  and  $+80$  mV, where  $\text{Cs}^+$  was the charge carrier from the *cis* to the *trans* side,  $\text{Zn}^{2+}$  applied to the *cis* side markedly reduced the  $\text{Cs}^+$  current.

(Fig. 5, B-2 and B-3). Thus,  $\text{Zn}^{2+}$  is more effective as a directional blockade when applied to the side from which the MVs fuse to the bilayer.

### MV $\text{Ca}^{2+}$ channel activity is modulated by GTP

Having found that ATP stimulated the MV  $\text{Ca}^{2+}$  channel activity, we also tested the effects of another nucleotide. GTP was chosen for study because it is known to be involved in ion channel regulation via interaction with G-proteins. We found that GTP evoked profound changes in MV  $\text{Ca}^{2+}$  channel characteristics (Fig. 6). Preincubation of



**FIGURE 6** Change in MV channel activity after preincubation with GTP. TCRMVs were incubated for several hours at room temperature in a 200 mM CsHEPES solution that contained 1 mM GTP and then were allowed to fuse to the PS:PE bilayers separating symmetrical 200 mM CsHEPES solutions for both the *cis* and *trans* compartments. Cs<sup>+</sup> currents were measured at a wide range of transmembrane potentials from  $-100$  mV to  $+80$  mV (A). Pooled single-channel current data from the different potentials of seven successful TCRMV channel incorporations were plotted against transmembrane potential (B). The straight line represents a linear least-squares fit of the points ( $i = \gamma \cdot V + i_0$ ), where  $i$  in pA represents the mean value of the single-channel current obtained from the corresponding amplitude histogram (C),  $i_0$  in pA is the intercept, and  $V$  in mV is the transmembrane potential. Under these conditions the single-channel conductance  $\gamma$  was  $22.5 \pm 2.2$  pS (mean  $\pm$  SD, 18 values). The single-channel current amplitude histogram is shown in C. The *inset* shows in detail a small segment of the channel activity. Mean amplitude of the current:  $-3.17$  pA at  $-100$  mV;  $\gamma = 32$  pS.

TCRMVs with GTP at room temperature ( $\sim 22^\circ\text{C}$ ) for 30–60 min greatly modified channel activity, changing it from irregular to extremely regular, with well-defined channel events. Fig. 6 A depicts a set of records at different transmembrane potentials acquired using a symmetrical 200

mM CsHEPES solution system (Cs<sup>+</sup> as the charge carrier). Recall that under normal conditions, the channels are open most of the time, displaying a behavior that reflects many different levels of conductance. In contrast, after incubation with GTP in both the *cis* and *trans* compartments, the channels remained closed for long periods of time and had only sporadic channel openings. It is clear from Fig. 6 A that the current levels were stabilized for definite periods of time, indicating preferred single-conductance states of the channels. The data shown in Fig. 6 A are selected segments of single-channel current records from an experiment to determine a single-channel conductance value.

Fig. 6 B presents a plot of the single-channel current-voltage relationship obtained from data collected from seven different incorporations. The straight line is the best fit of the data; it has a slope of  $22.5 \pm 2.2$  pS (mean  $\pm$  SD,  $n = 18$ ) and represents the conductance of a single cation channel ( $\gamma$ ). It is also apparent from Fig. 6 A that channel openings occurred in bursts. As illustrated in more detail by the inset in Fig. 6 C, the opening event included rapid transitions from the open to the closed state, giving the classical appearance termed “channel bursting.” The amplitude histogram, also shown in Fig. 6 C, was obtained from a single burst lasting  $\sim 2$  s. Note that the size of the conductance estimated from the histogram mean amplitude is  $\sim 32$  pS, somewhat larger than that estimated from the linear plot in Fig. 6 B. Indeed, as documented in the next section, multiconductance levels were frequently observed.

### Ca<sup>2+</sup> channels of other MV preparations are also modulated by GTP

The effects on channel activity of HCRMVs preincubated with GTP added to both the *cis* and *trans* compartments are shown in Fig. 7 A. Similar to the TCRMV pattern seen in Fig. 6, after exposure to GTP, HCRMV channels remained closed for long periods of time and exhibited sporadic openings with stabilized preferred conductance levels. The three predominant levels, indicated by the horizontal lines in Fig. 7 B, are evident in the single-channel current events recorded after GTP treatment. The corresponding amplitude histogram (Fig. 7 C) shows the predominant frequencies of occurrence of these conductance levels, the two most common ones being at 22 and 19 pS, and a less common one at 17 pS.

### ATP evokes MV channel flickering between GTP-induced preferred conductance levels

Because ATP and GTP had such different effects on the Ca<sup>2+</sup> channel activity of the MVs, we also examined the interaction that occurs when ATP is added to a preparation of GTP-stabilized MVs. Fig. 8 shows what happened to the channel activity when ATP (2 mM) was added to TCRMVs after they had been preincubated with GTP (1 mM). Fig. 8 A depicts the activity of a typical MV channel, incorporated

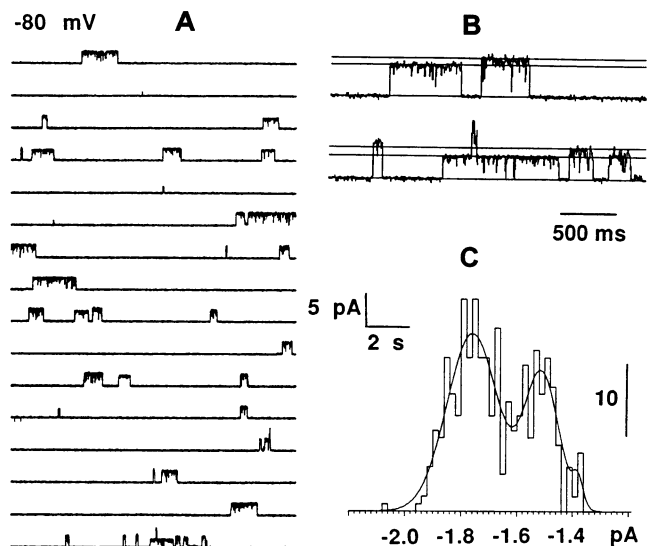


FIGURE 7 Effect of GTP on HCRMV channel activity. As with the previous MV preparation, the HCRMVs were incubated for several hours at room temperature in a 200 mM CsHEPES solution that contained 1 mM GTP and then were allowed to fuse to the PS:PE bilayers separating a symmetrical system with 200 mM CsHEPES solutions in both the *cis* and *trans* compartments. (A) Long (3.5 min) continuous recording of the channel activity generated by a transmembrane potential of  $-80$  mV. (B) Two segments of the channel activity to illustrate on an expanded time scale the presence of different single-channel current levels. (C) A 415-event amplitude histogram fitted by a trimodal Gaussian distribution showing mean values equal to  $-1.76$ ,  $-1.51$ , and  $-1.38$  pA. The corresponding conductance values for this HCRMV preparation were 22, 19, and 17 pS, respectively.

after exposure to GTP (i.e., low frequency of openings and preferred conductance levels). Records in Fig. 8, B–D, were sequentially acquired after the addition of ATP (2 mM) to both the *cis* and the *trans* sides of the bilayer. Segments indicated by the numbered bars are depicted below on an expanded time scale. Segment A1 illustrates the effect of GTP on a single MV channel activity with a conductance of  $\sim 25$  pS. Records B2, D3, and D4 were made at  $-20$  and  $60$  mV, respectively, illustrating the effects of ATP on the GTP-modulated MV  $\text{Ca}^{2+}$  channel activity. These records show that the channel becomes more active, exhibiting frequent incomplete openings. Mixed with this flickering current, one can still observe the characteristic stabilized, regular opening of the GTP-modified channel.

### Comparative effects of GTP on annexin V and MV $\text{Ca}^{2+}$ channel activity

Previous studies with highly purified annexin V incorporated into bilayer membranes formed at the tip of a patch pipette (Rojas et al., 1990, 1992; Berendes et al., 1993; Demange et al., 1994) had established that the annexin V  $\text{Ca}^{2+}$ -selective channel exhibits rapid transitions between multiple conductance levels, as described here for MV. The question we next asked was: Does GTP modulate the re-

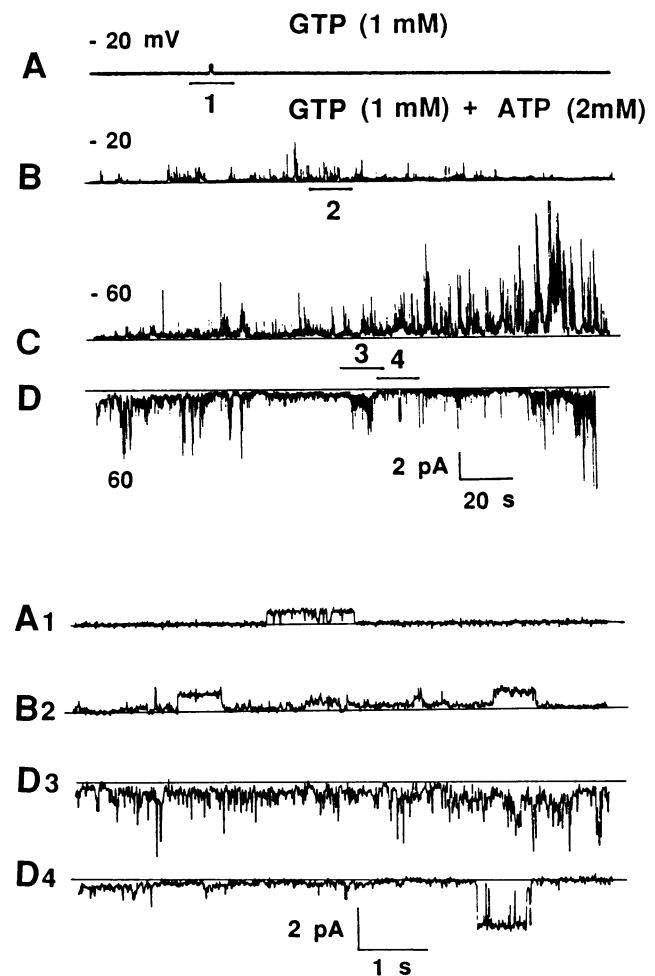
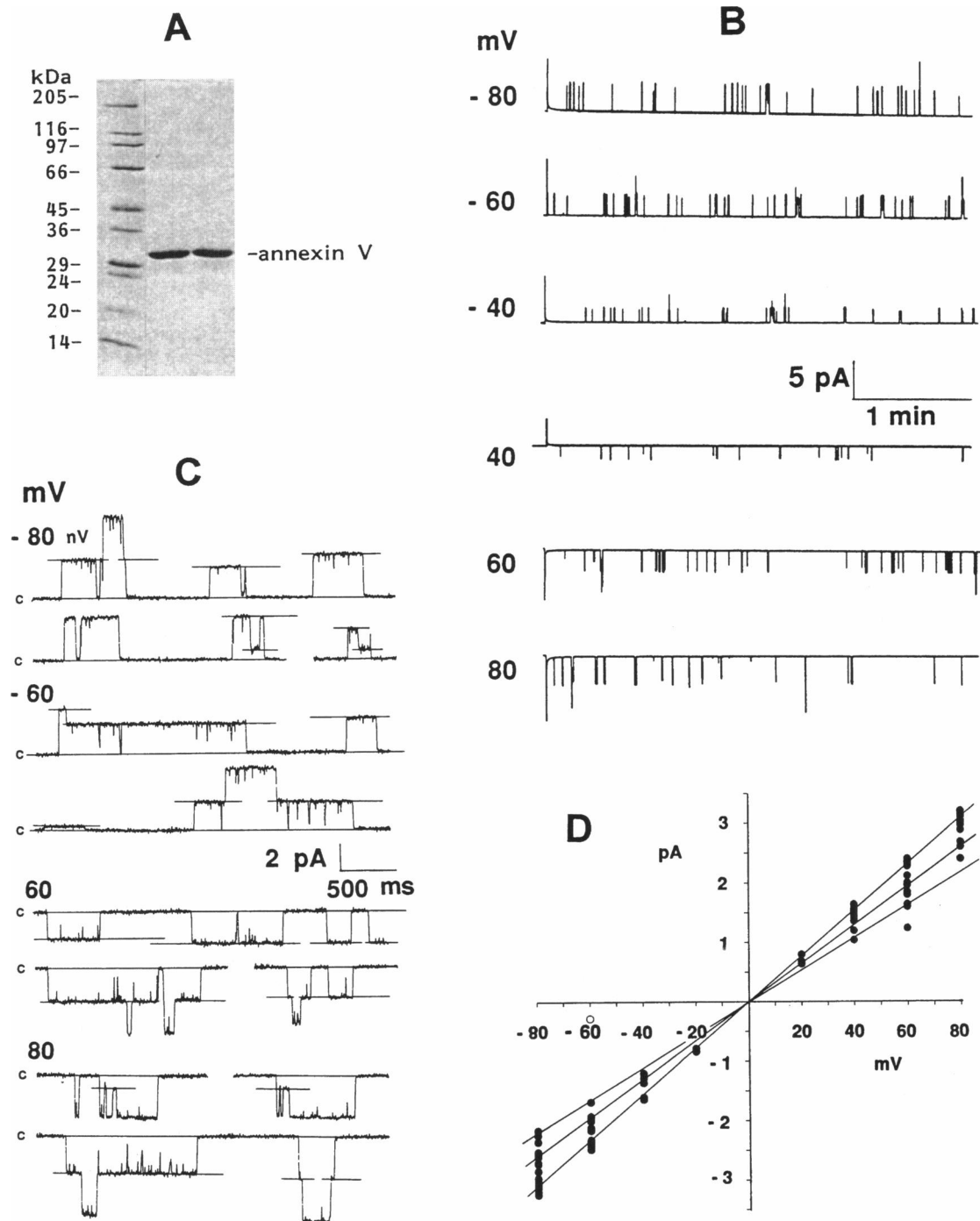


FIGURE 8 Effect of ATP on GTP-transformed TCRMV  $\text{Ca}^{2+}$  channels. TCRMV channel activity was transformed by incubation with GTP (1 mM) in the presence of 200 mM CsHEPES, as described in Fig. 7, and then the MV were fused with the PS:PE bilayer separating symmetrical 200 mM CsHepes solutions. Channel activity was first recorded in the presence of GTP (1 mM) before the addition of ATP (2 mM). (A) Current channel activity for a transmembrane potential of  $-20$  mV in the presence of GTP (1 mM) alone. Two minutes after the addition of ATP (2 mM), the current activity was again recorded at  $-20$  mV (B), at  $-60$  mV (C), and at  $60$  mV (D). Records A-1, B-2, D-3, and D-4 display, on an expanded time scale to show greater detail, regions taken from records A, B, and D at the times specified by the position of the numbered bars. Note in A-1 a sporadic stabilized bursting event, typically observed in the presence of GTP. Within a few minutes after exposure to ATP (B-2), an additional flickering multiconductance current activity appeared. With longer exposure to ATP and at increasing transmembrane potentials there is an increasing amplitude of the irregular current (D-3), although there remain isolated regions showing GTP-stabilized opening events (D-4).

constituted avian annexin V  $\text{Ca}^{2+}$ -selective channel in the same manner as the MV channel?

Fig. 9 summarizes our findings using highly purified avian annexin V. An SDS-PAGE gel of the avian annexin V used in our studies is shown in Fig. 9 A. Liposomes containing this annexin V were preincubated with GTP (1 mM) before insertion into the lipid bilayer. As shown in Fig. 9 B, after this treatment well-defined single-channel opening and



**FIGURE 9** Effect of GTP on Ca<sup>2+</sup> channel activity reconstituted from highly purified chicken annexin V. (A) Example of SDS-PAGE analysis of the highly purified preparation of avian annexin V used in these studies; previous studies with monospecific antibodies (Genge et al., 1990) had demonstrated the homogeneity of this protein. SDS-PAGE (Laemmli, 1970) was carried out using a 7.5–15% (w/v) gradient polyacrylamide gel stained with Coomassie blue. Left lane, MW standards; Center and right side lanes, avian annexin V (33 kDa). A sample (6–12  $\mu$ l) of the suspension containing the pure annexin V protein and the PS liposomes was added to the *cis* side of the chamber and incubated for 2 h in 200 mM CsHEPES solution containing 2 mM GTP. Then vesicles were allowed to fuse to a planar bilayer separating the *cis* and *trans* compartments, each containing 200 mM CsHEPES solution. Annexin V channel currents were then measured over extended periods of  $\sim$ 3.5 min (B) to obtain a statistically relevant assessment of variation in conductance levels and frequency of opening events at the six transmembrane potentials indicated in millivolts on the left next to the corresponding record. Activities from selected annexin V channel opening events at four different transmembrane potentials ( $-80$ ,  $-60$ ,  $+60$ , and  $+80$  mV) are displayed on expanded time and current scales in C. The current-voltage relationships for the different levels of current measured are shown in D. The lines were drawn using the three principal conductances obtained from amplitude histograms (not shown) constructed from current records at  $-60$  and  $-80$  mV. The following slope conductances were calculated from the data presented in B, C, and D:  $27 \pm 1$  (33),  $33 \pm 2$  (79), and  $39 \pm 2$  pS (120) (mean  $\pm$  SD (number of events)).



closing events were apparent. The channel kinetics were quite insensitive to changes in transmembrane potential, i.e., the number of events per unit time was unaffected by the potential level. A limited number of conductance states were evident from the series of annexin V channel current events recorded at the different transmembrane potentials. Fig. 9 C presents, on an expanded time scale to illustrate the multiple levels of current observed, selected events at different potentials. (Note that there were occasional two-channel opening events in this series of recordings.) From these data, single-channel current values at different transmembrane potentials were calculated. Fig. 9 D shows a current/voltage plot of data from these different experiments. Three straight lines were drawn to fit a series of single-channel current levels obtained from amplitude histograms at  $-60$  and  $-80$  mV (not shown). Means  $\pm$  SD of the single-channel conductance values in pS ( $27.4 \pm 1.3$  [33];  $33.2 \pm 1.9$  [79];  $39.3 \pm 1.9$  [120], [no. of events]) were obtained. These values, although consistent with those observed in MVs (Fig. 7), are higher, suggesting that other factors may decrease the conductance of the annexin V channel in the MV membrane.

Finally, to make a more direct comparison of the channel characteristics of the different MV preparations, and of annexin V, currents of the GTP-modified channels were recorded for extended periods of time (3–4 min) at either  $-60$  or  $-80$  mV and were illustrated at the same time and amplitude scales (Fig. 10). The channel activities observed for GTP-treated HCRMVs at  $-60$  mV (Fig. 10 A) or TCRMVs at  $-80$  mV (Fig. 10 B), and for GTP-treated liposomes containing avian annexin V at  $-60$  mV (Fig. 10 C) and at  $-80$  mV (Fig. 10 D) are all similar. However, although the intraburst kinetics were very similar, the single-channel conductance levels ( $\gamma$ ) of the MVs were only about three-fifths those of pure annexin V. In addition, the open probability,  $p_o$ , of the  $\text{Ca}^{2+}$  channel was substantially smaller when GTP-treated MVs, rather than GTP-treated liposomes containing annexin V, were allowed to fuse with the bilayer. These findings again suggest that other factors within the native MV membrane, but not present in the artificial liposomes, may be affecting the conductance level and kinetics of the annexin V channels studied in the bilayers.

## DISCUSSION

Previous findings had pointed to the likelihood that the annexins serve as  $\text{Ca}^{2+}$ -selective channels for  $\text{Ca}^{2+}$  loading during the induction of mineral formation by MVs. We present here for the first time direct evidence supporting this hypothesis.

### Annexin V forms a functional $\text{Ca}^{2+}$ -selective channel in MV

Several lines of evidence presented here strongly indicate that annexin V forms a  $\text{Ca}^{2+}$ -selective channel that func-

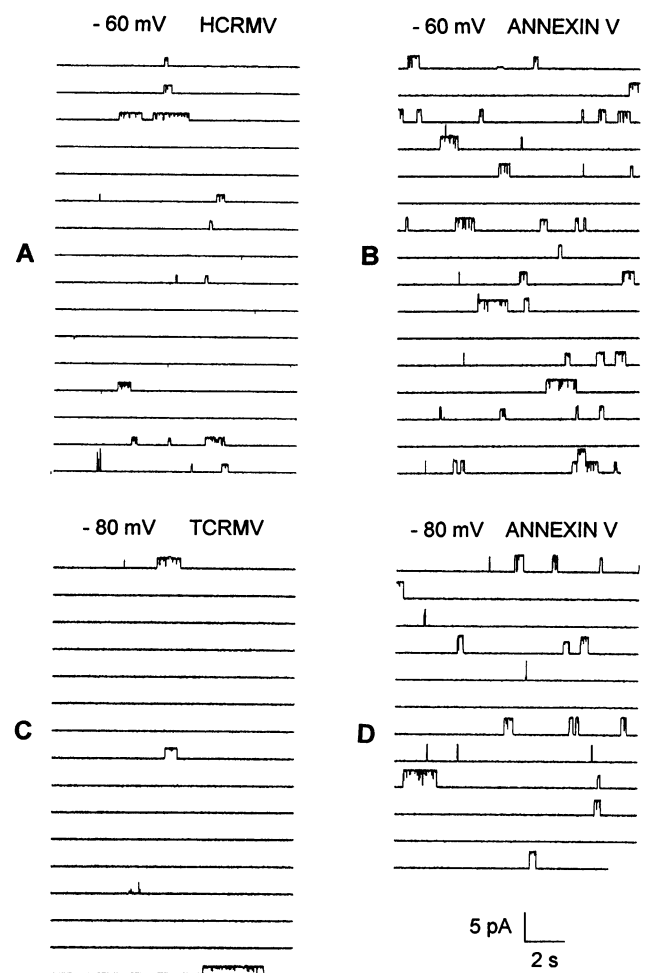


FIGURE 10 Comparison of the effects of GTP on MV and annexin V cation channel activity. Long-duration ( $\sim 3$ – $4$  min) recordings of cation channel activity obtained from MV (HCRMV and TCRMV) and annexin V, all treated with GTP under the same ionic conditions (symmetrical 200 mM CsHEPES), are displayed for comparison. Note that very similar and well-defined opening events and current levels were seen when both MV and annexin V preparations were incubated with GTP. However, for equivalent potentials, the well-defined current levels were significantly lower, and there were fewer openings, in the MV preparations (left) compared to those using pure annexin V (right).

tions in avian MVs. First, when MVs prepared either by trypsin-collagenase digestion (TCRMVs) or by hyaluronidase-collagenase digestion (HCRMVs) were incorporated into planar phospholipid bilayers, the  $\text{Ca}^{2+}$ -channel activities measured were very similar to those observed when pure annexin V-containing liposomes were allowed to fuse with identical bilayers. Some of the characteristic features of this  $\text{Ca}^{2+}$  channel activity, seen in both the native MVs as well as the artificial annexin V-liposome system, are 1) the rather complex channel kinetics consisting of multilevel bursts of channel open and close events, 2) the presence of several levels of single-channel conductance, and 3) the overall highly irregular activity.

Second,  $\text{Zn}^{2+}$ , a powerful inhibitor of  $\text{Ca}^{2+}$  uptake by MVs when assayed for mineral induction (Sauer et al.,

1989; Sauer and Wuthier, 1992), also blocks the Ca<sup>2+</sup>-selective channel activity resulting from the fusion with planar lipid bilayers of either MVs (current findings) or annexin V-containing liposomes (Rojas et al., 1992). Regarding the apparent discrepancy in the levels of Zn<sup>2+</sup> needed to block the annexin V channel and MV Ca<sup>2+</sup> uptake, the critical factor appears to be the ratio of Zn<sup>2+</sup> to Ca<sup>2+</sup>. In the MV ion uptake studies, Ca<sup>2+</sup> levels were 2 mM and required only 5–10  $\mu$ M Zn<sup>2+</sup> for complete inhibition (Sauer et al., 1989). In the annexin V ion-channel studies reported here, only when Ca<sup>2+</sup> levels were 70 mM was 1–2 mM Zn<sup>2+</sup> needed. It appears that Zn<sup>2+</sup> binds with higher affinity than Ca<sup>2+</sup> to the annexin V; thus a ratio of only about one Zn<sup>2+</sup> to 70 Ca<sup>2+</sup> ions is needed to block channel activity.

Third, the profound effects of GTP on the conductance of MV Ca<sup>2+</sup> channels are extremely similar to those seen on pure annexin V Ca<sup>2+</sup> channels. The striking similarities in the effects of GTP on native MV Ca<sup>2+</sup> channel activity and that of the reconstituted annexin V–liposome system provide strong evidence for identification of annexin V as the Ca<sup>2+</sup> channel present in the MV membrane. In fact, recent studies (Kirsch and Wuthier, 1994; Kirsch et al., 1994) on the stimulating effects of type II and X collagen on Ca<sup>2+</sup> uptake by MVs have been attributed to the well-known binding of these cartilage-specific collagens to annexin V (Mollenhauer et al., 1983, 1984; Wu et al., 1989, 1991). These findings, obtained with a very different experimental approach, taken with the results of our current studies, provide further evidence that Ca<sup>2+</sup> loading in MV occurs via annexin V. The annexins appear to be a new class of Ca<sup>2+</sup> channels that are normally resident in the cytosol but can become inserted in the cell membrane when cellular [Ca<sup>2+</sup>] increases.

### **MV Ca<sup>2+</sup>-selective channel is modulated by nucleotides**

One of the most exciting findings of this study is that the MV Ca<sup>2+</sup> channel is sensitive to nucleotides. GTP, when allowed to incorporate into annexin V before it was inserted into the membrane, caused a remarkable change in the channel activity of the protein from irregular to highly regular. Activity became organized into sporadic openings during which the open channel current remained stable at one of a small number of preferred levels. The conductances of the most frequently observed events in the annexin V channel were at  $39 \pm 2$  and  $33 \pm 2$  pS, but a conductance at  $27 \pm 1$  pS was also seen. It is significant that these conductance levels are proportionate to the three levels seen with GTP-modified TCRMVs in Fig. 8, and are similar to the lower conductance levels of the unmodified TCRMVs (Fig. 1). The GTP-binding site in annexin V appears to be highly specific: 1) it takes a long time (i.e.,  $\sim 1$  h) for the GTP to become incorporated; 2) GTP- $\gamma$ S failed to alter the channel activity, indicating that requirements for binding

must be very precise; and 3) ATP apparently binds to a different site (see next section).

ATP, added to the GTP-modulated MV channel, within minutes evoked a marked increase in channel activity. The characteristics of this combined nucleotide-modulated system were complex, showing a mixture of both types of channel behavior. Inasmuch as the current activity being measured was that from a single protein molecule, it is evident that there must be two different nucleotide binding sites on the annexin. GTP binding to one site must stabilize the cation channel to a reduced number of conformations that have well-defined open and closed states and conductance levels. These correspond closely to the lowest conductance states seen in the unmodified protein. ATP binding to the other site must relax the conformation of the protein, allowing a much wider range of conformations that have more active but less well-defined channel activity. When both nucleotide-binding sites are occupied, the conductance properties of the annexin V cation channel are a hybrid of the two. This also indicates that there must be two separate nucleotide-binding sites.

It is important to note that the effects of GTP on both the MV and the annexin V–liposome systems were nearly identical. Taken together with the antagonistic action of ATP on Zn<sup>2+</sup>-evoked Ca<sup>2+</sup> channel blockade, this provides further direct evidence that annexin V, the common factor in these two systems, is the Ca<sup>2+</sup> influx channel. The close similarity of all of these features, plus the fact that annexin V is a major protein in MVs, structures noted for their ability to accumulate massive amounts of Ca<sup>2+</sup> during the induction of mineral formation, led us to conclude that annexin V is the principal Ca<sup>2+</sup> channel in these structures.

However, other factors may be involved in the insertion, anchoring, and modulation of the activity of annexin V in the MV membrane. This is supported by the fact that although the general characteristic of the MVs and annexin V channel (the irregular pattern of channel events, the responses to Zn<sup>2+</sup> and GTP) are very similar, the conductances and open times of the two preparations were quantitatively different. This behavioral difference is most reasonably explained by constitutive differences in the two systems. For example, there is a more complicated pattern of lipids in MV than in the liposomes; whereas both contain PS and PE, MVs also contain large amounts of free cholesterol and sphingomyelin, which may stiffen the area near the inserted vesicles and could affect the conductance state of the incorporated annexin. In addition, there are other lipid-dependent Ca<sup>2+</sup>-binding proteins, including annexins II and VI, in MVs. These proteins may also modulate the channel activity of the annexin V inserted from the MV membrane.

The current discovery of the role of the nucleotides in modulating the cation channel activity is particularly exciting because of the profound effects they have on both the MVs and isolated annexin V cation channels. The full implications of these findings are difficult to ascertain at this time; however, it is of interest that for annexin V to insert into the plasma membrane and form a Ca<sup>2+</sup> channel,

cytosolic  $[Ca^{2+}]$  would have to be elevated above the normal resting state. In cells with normal levels of nucleotides, annexin V would have the opportunity to bind to both GTP and ATP; thus when elevations in  $[Ca^{2+}]$  occurred, the annexin upon insertion into the membrane would allow an influx of  $Ca^{2+}$  governed by the ratio of the two nucleotides present. In cells with depleted nucleotides, annexin V channel activity would likely be greater if transient elevations in cellular  $[Ca^{2+}]$  occurred. It is important to note that hypertrophic chondrocytes of the growth plate are nearly depleted of nucleotide triphosphates (Pollesello et al., 1991; Conklin and Bourne, 1993; Wuthier, 1993). Recent studies have shown that these cells frequently have elevated levels of cytosolic  $Ca^{2+}$  (Wu et al., 1996). Furthermore, there is evidence of massive influx in  $Ca^{2+}$  into the periplasmic region beneath the plasma membrane of these cells when they exfoliate large numbers of MVs (Wuthier, 1993; Wu et al., 1996). Thus nucleotide levels in chondrocytes appear to be a significant factor in modulating  $Ca^{2+}$  channels in the plasma membrane of these cells.

In conclusion, we have gathered strong evidence indicating that annexin V is a  $Ca^{2+}$ -selective, voltage-independent channel present in MVs. We also show here for the first time that biologically relevant substances, such as  $Zn^{2+}$ , ATP, and GTP, can profoundly modulate both channel gating and conductance. Thus, our data provide a basis for attributing a specific role to annexin V in calcification (Raynal and Pollard, 1994).

Thanks are given to Dr. H. B. Pollard for many illuminating discussions and to Burt Chidakel for electronic design and construction.

This work was supported in part by grant AR-18983 to REW from the National Institute of Arthritis and Musculoskeletal and Skin Diseases. NA was supported by the Cystic Fibrosis Foundation.

## REFERENCES

- Anderson, H. C. 1969. Vesicles associated with calcification in the matrix of epiphyseal cartilage. *J. Cell Biol.* 41:59–72.
- Arispe, N., H. B. Pollard, and E. Rojas. 1992. Calcium-independent  $K^+$ -selective channel from chromaffin granule membranes. *J. Membr. Biol.* 130:191–202.
- Berendes, R., D. Voges, P. Demange, R. Huber, and A. Burger. 1993. Structure-function analysis of the ion channel selectivity filter in human annexin V. *Science.* 262:427–430.
- Bewley, M. C., C. M. Boustead, J. H. Walker, D. A. Waller, and R. Huber. 1993. Structure of chicken annexin V at 2.25-Å resolution. *Biochemistry.* 32:3923–3929.
- Bonucci, E. 1970. Fine structure and histochemistry of "calcifying globules" in epiphyseal cartilage. *Z. Zellforsch. Mikrosk. Anat.* 103:192–197.
- Brecevic, L., and H. Füredi-Milhofer. 1972. Precipitation of calcium phosphates from electrolyte solutions. II. The formation and transformation of the precipitates. *Calcif. Tissue Res.* 10:82–90.
- Burger, A., D. Voges, P. Demange, C. R. Perez, R. Huber, and R. Berendes. 1994. *J. Mol. Biol.* 237:479–499.
- Cao, X., B. R. Genge, L. N. Y. Wu, W. R. Buzzzi, R. W. Showman, and R. E. Wuthier. 1993. Characterization, cloning and expression of the 67-kDa collagen-binding annexin from chicken growth plate cartilage matrix vesicles. *Biochem. Biophys. Res. Commun.* 197:556–561.
- Conklin, B. R., and H. R. Bourne. 1993. Structural elements of G-alpha subunits that interact with G-beta gamma receptors and effectors. *Cell.* 73:631–641.
- Demange, P., D. Voges, J. Benz, S. Liemann, P. Gottig, R. Berendes, A. Burger, and R. Huber. 1994. Annexin V: the key to understanding ion selectivity and voltage regulation? *Trends Biochem. Sci.* 19:272–276.
- Genge, B. R., X. Cao, L. N. Y. Wu, Y. Ishikawa, and R. E. Wuthier. 1992. Establishment of the primary structure of the two major matrix vesicle annexins by peptide and DNA sequencing. *J. Bone Miner. Res.* 7:807–819.
- Genge, B. R., G. R. Sauer, L. N. Y. Wu, F. M. McLean, and R. E. Wuthier. 1988. Correlation between loss of alkaline phosphatase activity and accumulation of calcium during matrix vesicle-mediated mineralization. *J. Biol. Chem.* 263:18513–18519.
- Genge, B. R., L. N. Y. Wu, H. D. Adkisson, and R. E. Wuthier. 1991. Matrix vesicle annexins exhibit proteolipid-like properties: selective partitioning into lipophilic solvents under acidic conditions. *J. Biol. Chem.* 266:10678–10685.
- Genge, B. R., L. N. Y. Wu, and R. E. Wuthier. 1989. Identification of phospholipid-dependent calcium-binding proteins as constituents of matrix vesicles. *J. Biol. Chem.* 264:10917–10921.
- Genge, B. R., L. N. Y. Wu, and R. E. Wuthier. 1990. Differential fractionation of matrix vesicle proteins: further characterization of the acidic phospholipid-dependent Ca-binding proteins. *J. Biol. Chem.* 265:4703–4710.
- Hsu, H. H. T. 1992. Further studies on ATP-mediated  $Ca^{2+}$  deposition by isolated matrix vesicles. *Bone Miner.* 17:279–283.
- Huber, R., J. Roemisch, and E. P. Paques. 1990. The crystal and molecular structure of annexin V, an anticoagulation protein that binds to calcium and membranes. *EMBO J.* 9:3867–3874.
- Kirsch, T., Y. Ishikawa, F. Mwale, and R. E. Wuthier. 1994. Roles of the nucleolar core complex and collagens (type II and X) in calcification of growth plate cartilage matrix vesicles. *J. Biol. Chem.* 269:20103–20109.
- Kirsch, T., and R. E. Wuthier. 1994. Stimulation of calcification of growth plate cartilage matrix vesicles by binding to type II and X collagens: apparent activation of annexin V  $Ca^{2+}$  channels. *J. Biol. Chem.* 269:11462–11469.
- Laemmli, U. K. 1970. Cleavage of structural proteins during the assembly of the head of bacteriophage T4. *Nature.* 227:680–685.
- McLean, F. M., P. J. Keller, B. R. Genge, S. A. Walters, and R. E. Wuthier. 1987. Disposition of preformed mineral in matrix vesicles. Internal localization and association with alkaline phosphatase. *J. Biol. Chem.* 262:10481–10488.
- Mollenhauer, J., J. A. Bee, M. A. Lizarbe, and K. von der Mark. 1984. Role of anchoring CII, a 31,000-mol-wt membrane protein, in the interaction of chondrocytes with type II collagen. *J. Cell. Biol.* 98:1572–1578.
- Mollenhauer, J., and K. von der Mark. 1983. Isolation and characterization of a collagen-binding glycoprotein from chondrocyte membranes. *EMBO J.* 2:45–50.
- Pollesello, P., B. de Bernard, M. Grandolfo, S. Paoletti, F. Vittur, and B. J. Kvam. 1991. Energy state of chondrocytes assessed by  $^{31}P$ -NMR studies of preosseous cartilage. *Biochem. Biophys. Res. Commun.* 180:216–222.
- Raynal, P., and H. B. Pollard. 1994. Annexins: the problem of assessing the biological role for a gene family of multifunctional calcium- and phospholipid-binding proteins. *Biochim. Biophys. Acta.* 1197:63–93.
- Register, T. C., G. P. Warner, and R. E. Wuthier. 1984. Effect of L- and D-tetramisole on  $P_i$  and Ca uptake and mineralization by matrix vesicle-enriched fractions from chicken epiphyseal cartilage. *J. Biol. Chem.* 259:922–928.
- Rojas, E., N. Arispe, H. T. Haigler, A. L. Burns, and H. B. Pollard. 1992. Identification of annexins as calcium channels in biological membranes. *Bone Miner.* 17:214–218.
- Rojas, E., H. B. Pollard, H. T. Haigler, C. Parra, and A. L. Burns. 1990. Calcium-activated endonexin II forms calcium channels across acidic phospholipid bilayer membranes. *J. Biol. Chem.* 265:21207–21215.
- Sauer, G. R., H. D. Adkisson, B. R. Genge, and R. E. Wuthier. 1989. Regulatory effect of endogenous zinc and inhibitory action of toxic metal ions on calcium accumulation by matrix vesicles in vitro. *Bone Miner.* 7:233–244.

- Sauer, G. R., and R. E. Wuthier. 1992. Influence of trace metal ions on matrix vesicle calcification. *Bone Miner.* 17:284–289.
- Valhmu, W. B., L. N. Y. Wu, and R. E. Wuthier. 1990. Effects of Ca/P<sub>i</sub> ratio, Ca<sup>2+</sup> × P<sub>i</sub> ion product, and pH of incubation fluid on accumulation of Ca by matrix vesicles in vitro. *Bone Miner.* 8:195–209.
- Wonderlin, W. F., R. J. French, and N. J. Arispe. 1990. Recording and analysis of currents from single ion channels. In *Neuromethods*, Vol. 14. A. A. Boulton, G. B. Baker, and C. H. von der Wolf, editors. Humana Press, Clifton, NJ. 35–142.
- Wu, L. N. Y., B. R. Genge, and R. E. Wuthier. 1991. Collagen binding proteins in collagenase-released matrix vesicles from cartilage: specific binding of annexins, alkaline phosphatase, link and hyaluronic acid binding region proteins to native cartilage collagen. *J. Biol. Chem.* 266:1195–1203.
- Wu, L. N. Y., G. R. Sauer, B. R. Genge, and R. E. Wuthier. 1989. Induction of mineral deposition by primary cultures of chicken growth plate chondrocytes in ascorbate-containing media: evidence of an association between matrix vesicles and collagen. *J. Biol. Chem.* 264:21346–21355.
- Wu, L. N. Y., M. G. Wuthier, B. R. Genge, and R. E. Wuthier. 1996. In situ levels of intracellular Ca<sup>2+</sup> and pH in avian growth plate cartilage. *Clin. Orthop.* In press.
- Wu, L. N. Y., T. Yoshimori, B. R. Genge, G. R. Sauer, T. Kirsch, Y. Ishikawa, and R. E. Wuthier. 1993. Characterization of the nucleational complex responsible for mineral induction by growth plate cartilage matrix vesicles. *J. Biol. Chem.* 268:25084–25094.
- Wuthier, R. E. 1988. Mechanism of matrix vesicle-mediated mineralization of cartilage. *ISI Atlas Sci. Biochem.* 1:231–241.
- Wuthier, R. E. 1993. Involvement of cellular metabolism of calcium and phosphate in calcification of avian growth plate cartilage. *J. Nutr.* 123:301–309.
- Wuthier, R. E., R. E. Linder, G. P. Warner, S. T. Gore, and T. K. Borg. 1978. Non-enzymatic isolation of matrix vesicles: characterization and initial studies on <sup>45</sup>Ca and <sup>32</sup>P-orthophosphate metabolism. *Metab. Bone Dis. Relat. Res.* 1:125–136.